FATIGUE PROPERTIES OF P/M MATERIALS

Robert C. O'Brien

Hoeganaes Corporation
River Road
Riverton, New Jersey 08077

Presented at the SAE Congress
Detroit, Michigan, February 29-March 4, 1988

Abstract

The tensile properties and fatigue endurance limits of several widely used P/M steels have been tested. Statistical estimates of the 99.9% survival stress have shown that fatigue endurance ratios can vary from 0.16 to 0.47. Thus the use of 0.38 as a rule of thumb for estimating the fatigue endurance limit from static tensile property data can result in large errors.

The single most effective method of improving fatigue properties is to increase the part density.

Fractographic observations were made on some of the fatigue failures, including stable and unstable crack growth.

Introduction

The choice of materials used in structural components designed to undergo cyclic loading must be made on the basis of fatigue strength. Although there is an extensive database on the static tensile properties of powder metallurgy (P/M) steels, parts designers have been forced to rely on rough estimates of fatigue endurance limits. Typically, a fatigue strength value of 38% of the static tensile strength has been used as a rule of thumb for P/M steels. (1, 2) A previous series of fatigue tests by the author has shown that this assumed fatigue endurance ratio (ratio of fatigue endurance limit to tensile strength) of 0.38 is often an overestimate. (3)

The objective of the present study was to provide close statistical estimates of the fatigue endurance limits of commonly used P/M steels. These data, combined with increasingly accurate analyses of the stress distributions in components subjected to cyclic loading, can allow parts designers to optimize the use of materials in high performance components where it is crucial that the weight of reciprocating parts be kept to a minimum, while their reliability is maintained.

The effects on fatigue properties of several process variables in the production of P/M parts have been evaluated. The process variables studied
were:

- Alloying Method
- Sintering Temperature
- Sintered Density
- Matrix Strength

Experimental

Materials

Specimens used in this study were prepared using iron-based powders with alloying additions made by three techniques, described below:

- Admixed steel powders: The alloy additions are made in the form of elemental powders. This is the least expensive and most commonly used alloying method. Since the iron powder base is unalloyed when the mix is pressed, admixed steels are highly compressible. The degree of alloying in admixed P/M steel is limited by the diffusivity of the alloying elements in iron at the sintering temperature, and the resulting microstructures are chemically heterogeneous. This type of mix is also subject to powder segregation during handling and pressing.

- Prealloyed steel powders: Alloying elements except for carbon are added to the melt before atomization. The problems of powder segregation and heterogeneous microstructure are thus eliminated; but solution hardening of the powder particles by the alloy additions decreases the compressibility of prealloyed steel mixes compared with that of admixed steels.

- Partially alloyed steel powders: Alloying additions are diffusion bonded to the base iron particles. The resulting powder mixes are highly compressible, and yield sintered microstructures consisting of low alloy particle cores with a continuous network of tough, highly alloyed interparticle bonds. Typical compositions of the prealloyed and partially alloyed steels used in the study are shown in Table 1.

Test Specimen Preparation

The mix compositions shown in Table 2 were blended with 0.5% lubricant unless noted. The lubricant was atomized ethylene bis stearamide wax, tradename Acrawax C, produced by Lonza, Inc. Copper was added as Alcan 8081; nickel as Inco 123. Asbury 3203 natural graphite was used. Tensile specimens were pressed according to MPIF Std. 10.

Sintering was carried out at 2050°F for 30 minutes at temperature in a dissociated ammonia (D.A.) atmosphere unless other processing is indicated in the sintered property tables. The samples were placed on a bed of alumina powder in a ceramic tray, and covered with more alumina powder to prevent decarburizing. Those specimens sintered at 2425°F were held at

Picture page 3

Picture page 4

temperature for 60 minutes, in a dissociated ammonia plus methane atmosphere. After sintering, the trays were pushed directly into a water jacketed cooling zone.

Specimens for heat treatment were austenitized in a muffle furnace using a D.A. atmosphere, with propane added to maintain carbon potential. The specimens were quenched in circulating synthetic oil coolant, which was preheated to 150°F. Tempering was done in air.

Testing

Tensile specimens were tested without machining. RBF specimens (Figure 1) were machined from 0.395" x 0.395" x 3" blanks.

The rotating bending fatigue specimens were loaded as shown in Figure 2 and tested at 3300 RPM, with survival to 10 million cycles considered a "run-out". Twenty specimens were used per test. Bending moments were chosen by the "staircase" method (4) until appropriate stress levels were determined for a two-point estimate of the fatigue endurance limit, which for the purposes of this study was defined as the 99.9% survival stress.

Results

The fatigue endurance limits of all materials tested are compared in Figure 3. Details on the individual data points in these figures are given in Tables 3 - 6.

Discussion

Fatigue Test Configuration

In the rotating bending fatigue test, an axial bending moment is placed on an hourglass-shaped section of the specimen (Figures 1 and 2). The Stress State of an element at the surface of the outer bend radius of this section approximates uniaxial tension. As the element rotates to the inner radius of the bend, this changes to a compressive stress equal in magnitude to the prior tensile state. The load cycle is thus sinusoidal, with a stress ratio $R = s_{min.}/s_{max}$ **of -1.**

Experience has shown that RBF tests give higher endurance limit results than axial tests on the same materials. Which test method is more applicable to part design is unclear. While axial fatigue tests are more flexible with respect to stress ratio and yield more conservative results, RBF tests often closely simulate the real life operating conditions of rotating parts. The fatigue endurance limit values determined in this study are estimates of the cyclic stress level at which 99.9% of the specimens would survive 10 million cycles.

Distribution of Fatigue Endurance Ratios

In Figure 3, the fatigue performance of all materials tested in the study is compared by plotting the fatigue endurance limit of each material against its tensile strength. Also included is a line showing the fatigue strength for any given tensile strength, assuming an endurance ratio of 0.38. It is apparent that fatigue performance cannot be estimated reliably from the tensile strength using this fixed ratio.

Materials Characteristics Controlling Fatigue Strength

Although processing plays a crucial role in fatigue performance, the endurance limits of the materials tested can be distinguished broadly by the alloying method used in the processing; as shown in Figure 4. The admixed copper and nickel steels which were not heat treated or high temperature sintered are clustered in the lower left quadrant of Figure 4a. The phosphorus steels as a class had relatively low tensile strengths, but high endurance ratios. The air hardening steels had high tensile strengths, but did not yield correspondingly high fatigue endurance limits.

The two fully prealloyed materials shown in Figure 4a were tested in the heat treated condition, and had relatively high tensile strengths and high fatigue endurance limits.

The steels made from partially alloyed powders are shown separately in Figure 4b. Depending on processing, they tend to be clustered toward the upper right, high performance end of the chart.

Processing Variables Controlling Fatigue Strength

The fatigue endurance limits of some of the materials were determined for various sintering temperatures and densities. The effect of sintered density on the fatigue properties was shown to be much greater than that of sintering temperature.

Sintering Temperature Effects

Sintering at 2300°F and above was expected to improve the all-around performance of the materials by spheroidizing the porosity, thereby decreasing the severity of the stress concentration around pores. The Distaloy 4600A with

Picture page 6

Picture Page 7

Picture page 8

0.6% graphite added did not act as predicted. As the sintering temperature was increased from 2050°F to 2300°F, the tensile strength increased from 98,900 psi to 106,300 psi, but the endurance limit decreased by 5,000 psi to 28,500 psi (Table 3). The same result was observed in Distaloy 4800A with 0.4% graphite: a small increase in tensile strength with higher sintering temperature, but a decrease in fatigue strength.

Picture page 9

The response of admixed steels to increased sintering temperature was a large increase in static tensile properties (Table 4). The tensile strength of FN-0208 increased from 64,500 to 83,600 psi on sintering at 2425°F. The tensile strength of FC-0208 also increased with high temperature sintering, to 112,700 psi. The fatigue strengths of the admixed steels showed substantial improvements with high temperature sintering, increasing from 22,220 psi to 31,200 psi for FN-0208, and from 34,000 psi to 39,000 psi for the FC-0208.

Picture page 10

Density Effects

Increasing the density by double pressing invariably resulted in increases in the tensile properties and fatigue strength. The tensile strength of double pressed Distaloy 4800A was 134,000 psi, compared with 103,000 psi for the single pressed materials (Table 3). The corresponding fatigue endurance limits were 44,000 and 37,000 psi. Table 5 shows that increasing the density of the 0.9% phosphorus steel with a double pressing step increased the fatigue endurance limit by 10,000 psi to 39,700 psi. The largest increase in endurance limit due to higher density occurred in the heat treated prealloyed steel (Table 6). The fatigue strength of Ancorsteel 4600V increased by 16,000 psi to 57,500 psi as the sintered density was increased to 7.25 g/cm^3 by double pressing. High density ~9cessing is the single most effective way of producing high fatigue strength in porous steels.

Picture page 11

Microstructural Effects

The air hardening steels (Table 4) are the most highly alloyed of the admixed materials tested. The specimens were stress relieved at 500°F after cooling from the sintering temperature, and had tempered martensitic microstructures with apparent hardness up to Rockwell C 27. The tensile strengths were accordingly high: up to 135,900 psi. However, the high tensile strength and hardness of the martensitic microstructures did not in this case produce particularly high fatigue strength: only 21,200 psi for the Ancorsteel 4600V-based air hardening steel, which had a fatigue endurance ratio of 0.16.

The response of low alloy steels to high temperature sintering is dependent on the method of alloy addition. For example, the microstructure of the Distaloy 4800A diffusion-bonded steel (Figure 5a) consisted of pearlitic particle cores surrounded by nickel-rich areas of martensite with retained austenite. The fatigue properties of this material are thought to benefit from the heterogeneity of its structure, which provides strong, tough high nickel areas to arrest fatigue cracks during stable growth. Increasing the sintering temperature or time at temperature will improve the pore shape; but if the nickel is more completely homogenized in the structure as shown in Figure 5b, the crack-arresting phase is lost.

Picture page 12

Thus, if the high temperature sintering cycle had been applied to a pre-alloyed material such as Ancorsteel 4600V, which is already chemically homogeneous before it is sintered, the benefits of pore rounding at high temperatures would probably be reflected in the fatigue properties as well as the tensile properties.

Observations on Fatigue Crack Growth

Fractography on failed fatigue specimens yielded information on the pattern of stable and unstable crack growth that was found to be typical of the rotating bending fatigue test.

Observations of stable fatigue cracks were also made. The choice of ten million cycles as the definition of a "runout" in this series of tests has resulted in some instances where tests on certain specimens were terminated while stable cracks were growing in the specimens. By sectioning in a plane normal to the crack, these could be examined.

RBF Failure Mode

The fractography of fatigue failures in fully dense materials is well established. (5) As a rule, the initiation site is at the surface of the part. During cycling, there follows a period of slow, stable crack growth, which typically lasts for ten million stress cycles in low alloy steels. As the crack grows in its stable mode, a point is reached where the stress around the crack tip has increased due to the length of the crack and the reduction in remaining cross sectional area, and the crack proceeds to failure in the course of a few stress cycles.

This failure mode has been found to apply to porous steels as well (6). Details on the pattern of stable and unstable crack growth in RBF specimens are given in the schematic of Figure 6. The crack initiates at the surface (Figure 6a) and proceeds radially inward in stable growth. The inward growth is halted as the stress at the crack tip decreases according to the profile in Figure 7; however, growth continues tangentially near the surface, where the stress is highest (Figure 6b). The tangential growth has been known to proceed in a stable mode until the two fronts meet at the other side of the specimen (Figure 6c).

Picture page 13

This growth pattern is unique to the RBF test configuration, and may be the reason that RBF testing appears to result in higher endurance limits than axial fatigue testing: rotating bending fatigue cracks must traverse a large portion of the circumference of the specimen, rather than just the diameter, as is the case for axial specimens.

The plane of a rotating bending fatigue crack in stable growth is characterized by smoothly worn surfaces produced by the rubbing together of the two faces of the crack during the compressive part of the load cycle. The unstable part of the fracture plane is typical of an axial tension failure. The transition between the two modes is very sharp, and both modes can be seen in a single metallographic field, as shown in Figure 8.

Picture page 14

Stable Crack Growth

The propagation path of cracks in stable growth through porous materials has been defined by examining cross sections of cracks that were in stable growth when the RBF test was halted. The cracks follow the path of least resistance that is provided by the pores, as shown in Figure 9. The crack ends in a pore, which blunts the tip (Figure 10).

Conclusions

Statistical estimates of the 99.9% survival stress have shown that fatigue endurance ratios of commonly used P/M steels can vary from 0.16 to 0.47. Thus the use of 0.38 as a rule of thumb for estimating the fatigue endurance limit from static

tensile property data can result in large errors.

The single most effective method of improving fatigue properties is to increase the part density.

Sintering at elevated temperatures increases the static tensile properties of the admixed and partially prealloyed steels, but did not always improve the fatigue properties of the partially alloyed steels, possibly because of loss of microstructural heterogeneity.

As suggested in the literature (5), porous steels should ideally be fatigue tested to 50 to 100 million cycles rather than ten million, since some samples, which were considered to be “runouts”, were found to have stable fatigue cracks growing in them.

Acknowledgement

The author would like to thank W. R. Bentcliff and R. J. Fitzpatrick for their help in mechanical property specimen preparation and testing; also Remington Arms for the 2,425°F sintering.

References

(1) A. F. Kravic, D. L. Pasquine, "Fatigue Properties of Sintered Nickel Steels", International Journal of Powder Metallurgy, 5 (1) 1969 p 55.

(2) "Materials Standards for P/M Structural Parts", MPIF Standard 35, Metal Powder Industries Federation, 1977-1988 Edition.

(3) R. C. O'Brien, "Impact and Fatigue Characterization of Selected Ferrous P/M Materials", Progress in Powder Metallurgy 1987, Vol. 43, Metal Powder Industries Federation, 1987, p 761.

(4) R. C. Rice, "Fatigue Data Analysis", ASM Metals Handbook, Vol. 8, 9th Edition, 1985, pp 695-720.

(5) R. Haynes, "Fatigue Behavior of Sintered Metals and Alloys", Powder Metallurgy, Vol. 13, No. 26, October 1980, pp 465-510.

(6) G. Dieter: Mechanical Metallurgy~ McGraw-Hill, New York, 1961, p 381.

Table 1: Typical Compositions of the Base Materials Used in the Mixes (Wt. %)

Name	Ni	Mo	Cu	Mn	C	O_2
Ancorsteel 1000B	--	--	--	0.10	<.01	0.08
Ancorsteel 4600V	1.80	0.50	--	0.25	0.02	0.13
Ancorsteel 2000	0.45	0.60	--	0.30	0.02	0.17
Distaloy 4600A	1.80	0.55	1.60	0.10	<.01	0.16
Distaloy 4800A	4.05	0.55	1.60	0.10	<.01	0.16

Table 2: Typical Mix Compositions (Wt. %).

Method of Alloy Addition	Name	Ni	Mo	Cu	Mn	P	Carbon Added as Graphite	Typical Sintered Carbon
Admixed * Low Alloy	FN-0208	2.00	--	--	0.10	--	0.75	0.67
	FC-0208	--	--	2.00	0.10	--	0.90	0.81
Admixed * Phosphorus	0.9% P +	--	--	--	0.10	0.90	0.18	0.21
	0.8% P	--	--	--	0.10	0.80	0.40	0.38
Prealloyed	Ancorsteel 4600V	1.80	0.50	--	0.25	--	0.60	0.54
Prealloyed with admixed elements "Air Hardening"	**	1.80	0.50	2.00	0.25	--	1.00	0.93
	***	0.45	0.60	2.00	0.30	--	1.00	0.94
Partially Alloyed	Distaloy 4600A	1.80	0.55	1.60	0.10	--	0.60	0.55
	Distaloy 4800A	4.05	0.55	1.60	0.10	--	0.60	0.55

* Base Iron: Ancorsteel 1000B + Added as Fe P
** Base Iron: Ancorsteel 4600V
*** Base Iron: Ancorsteel 2000

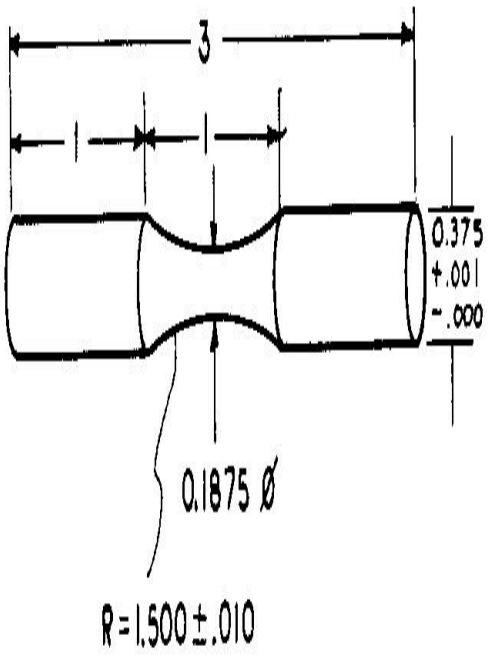

Figure 1: Rotating bending fatigue specimen.

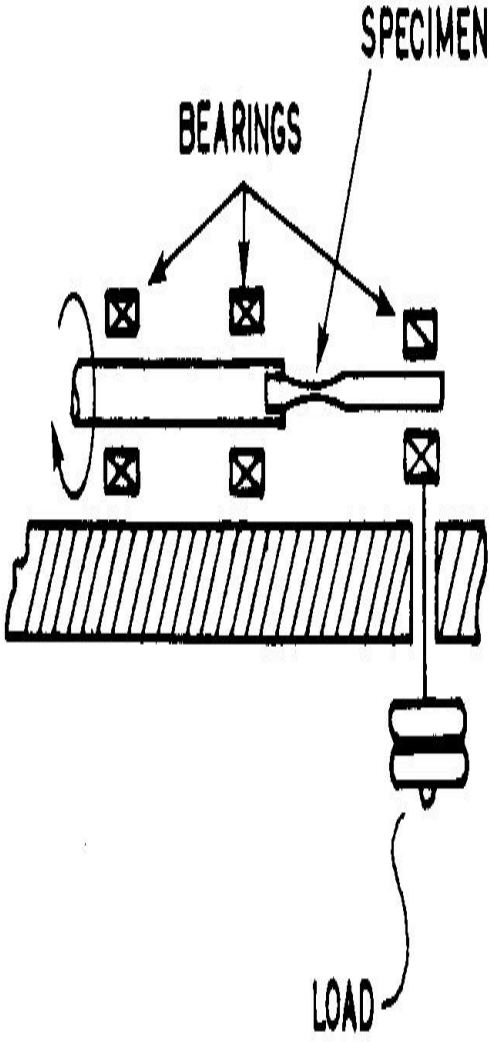

Figure 2: Loading configuration for rotating bending fatigue test.

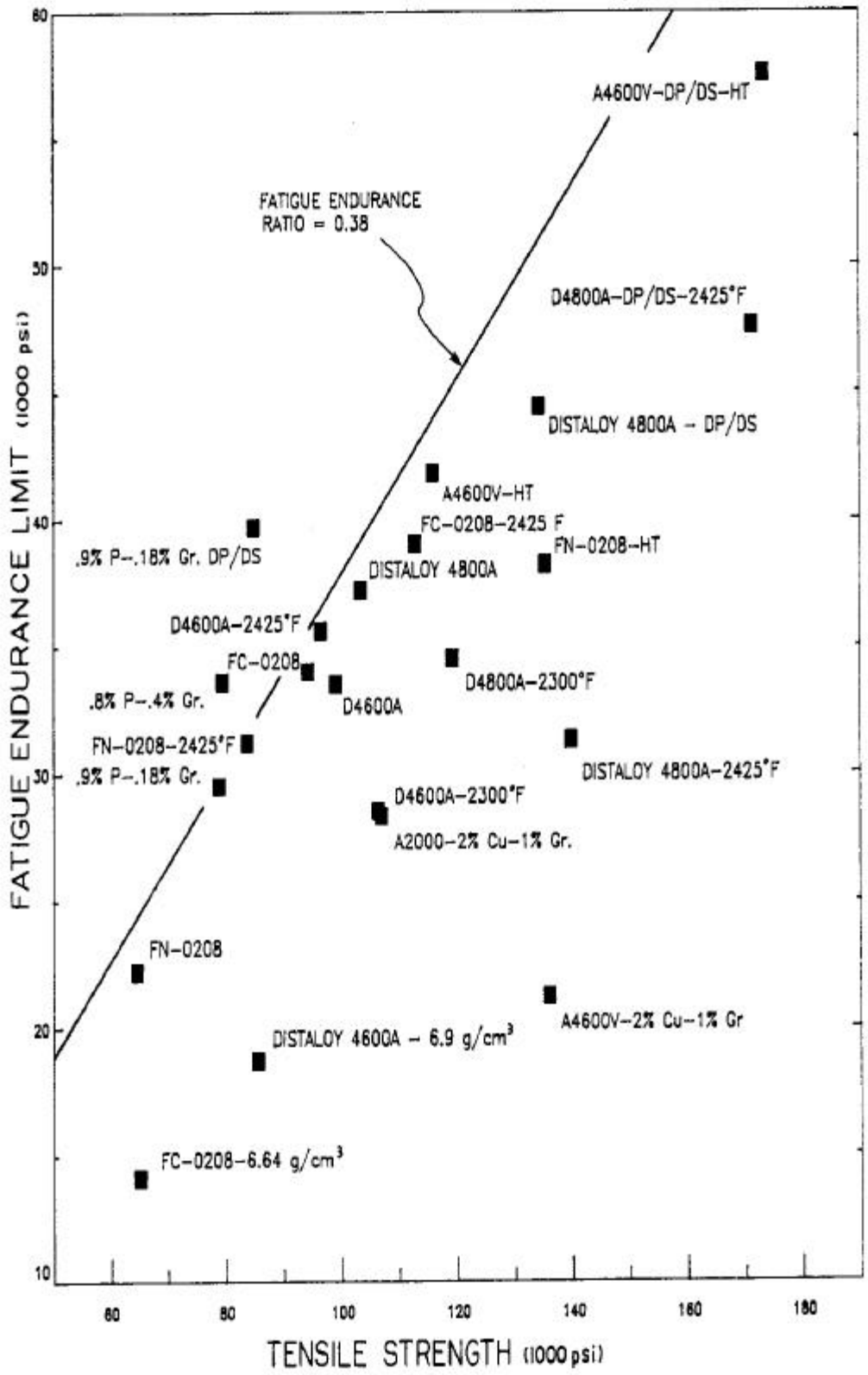

Figure 3: Fatigue endurance limits of all materials tested in this study, plotted against tensile strength.

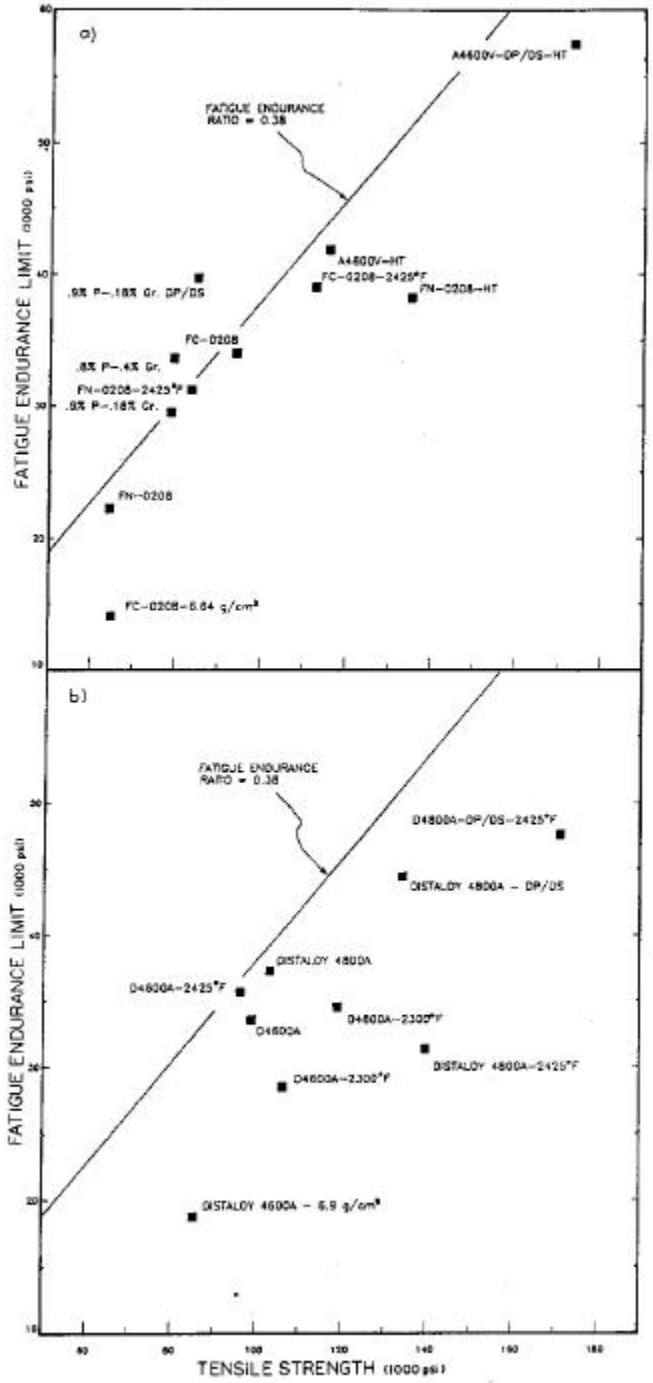

Figure 4: Fatigue endurance limits plotted against tensile strength: a) admixed steels and fully prealloyed steels. b) Partially alloyed steels.

Table 3: Fatigue Endurance Limits of Partially Alloyed Steels
Estimates of the 99.9% Survival Stress

MATERIAL, PROCESS		B.P. (TSI)	D.C. (%)	SINT. DENS. (g/cm^3)	RCKWL HRDNS	YIELD STRENGTH (psi)	TENSILE STRENGTH (psi)	% El. in 1"	ENDUR. LIM. (psi)	END. RATIO
DISTALOY 4600A										
Distaloy 4600A + 0.6% Gr.		45	+0.24	7.13	B 94	62,400	98,900	4	33,500	0.34
Same, 2300 F		45	+0.01	7.16	B 92	70,500	106,300	4	28,500	0.27
Same, 2425 F	*	45	-0.21	7.19	B 88	70,600	96,300	4	35,600	0.37
Distaloy 4600A + 0.6% Gr. -aim 6.9 g/cm^3		34	+0.14	6.87	B 86	60,800	85,460	3	18,700	0.22
DISTALOY 4800A										
Distaloy 4800A + 0.4% Gr.		50	--	7.20	B 92	63,500	103,200	4	37,200	0.36
Same, 2300 F		50	--	7.23	B 98	77,900	119,100	4	34,500	0.29
Distaloy 4800A 0.6% Gr. 2425 F	*	45	-0.40	7.20	C 28	98,700	139,700	2	31,300	0.22
Distaloy 4800A + 0.4% Gr. Double Pressed		50/50	+0.13	7.42	C 23	71,000	134,100	4	44,400	0.33
Distaloy 4800A 0.6% Gr. 2425 F Double Pressed	*	50/50	-0.10	7.43	C 32	105,700	171,200	2	47,600	0.28

Table 5: Fatigue Endurance Limits of Some Phosphorus Steels
Estimates of the 99.9% Survival Stress

MATERIAL, PROCESS	B.P. (TSI)	D.C. (%)	SINT. DENS. (g/cm^3)	RCKWL HRDNS	YIELD STRENGTH (psi)	TENSILE STRENGTH (psi)	% El. in 1"	ENDUR. LIM. (psi)	END. RATIO
0.8% P	50	--	6.94	B 81	59,600	79,400	5	33,600	0.42
0.9% P	50	+0.23	7.06	B 80	59,800	78,800	7	29,500	0.37
0.9% P-DP/DS *	50/50	+0.11	7.25	B 88	68,700	84,800	4	39,700	0.47

* Presintered at 1400 F for 30 minutes in D.A.

Table 6: Fatigue Endurance Limits of Heat Treated Prealloyed Steel
Austenitized 1550 F in D.A. for 30 min, oil quenched.
Tempered 450 F for 1 Hr. in air.

ALLOYING METHOD	B.P. (TSI)	D.C. (%)	SINT. DENS. (g/cm^3)	RCKWL HRDNS	YIELD STRENGTH (psi)	TENSILE STRENGTH (psi)	% El. in 1"	ENDUR. LIM. (psi)	END. RATIO
Ancorsteel 4600V + .6% Gr.	45	-0.25	6.96	C 26	No Yield	115,780	< 1	41,800	0.36
Same, DP-DS	45	-0.13	7.25	C 35	165,310	173,250	< 1	57,500	0.33

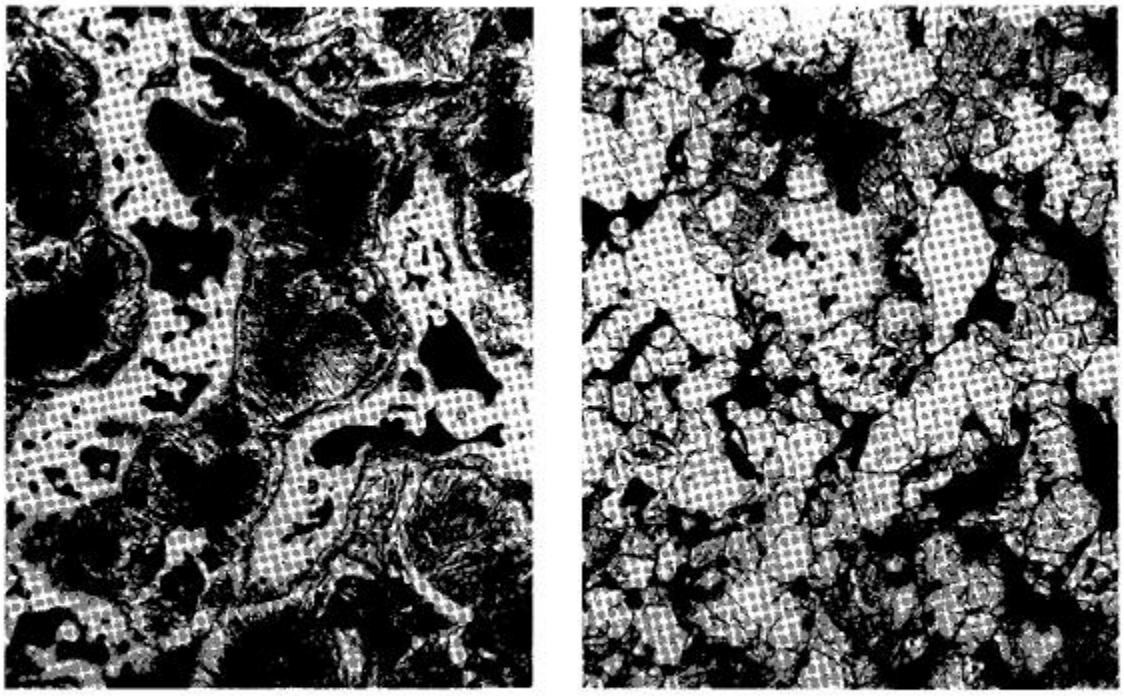

(a) (b)

Figure 5: Distaloy 4800A with 0.6% graphite. When sintered for 30 min. at 2050°F, the microstructure contains interparticle areas of tough high nickel martensite, which can arrest fatigue cracks (a). Homogenizing the nickel content during sintering removes these areas (b).
500X 2% Nital, 4% Picral

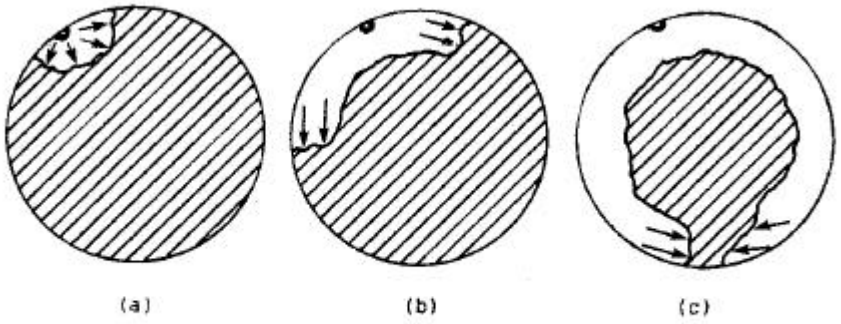

Figure 6: Stable fatigue crack growth pattern in the cross section of an RBF specimen.

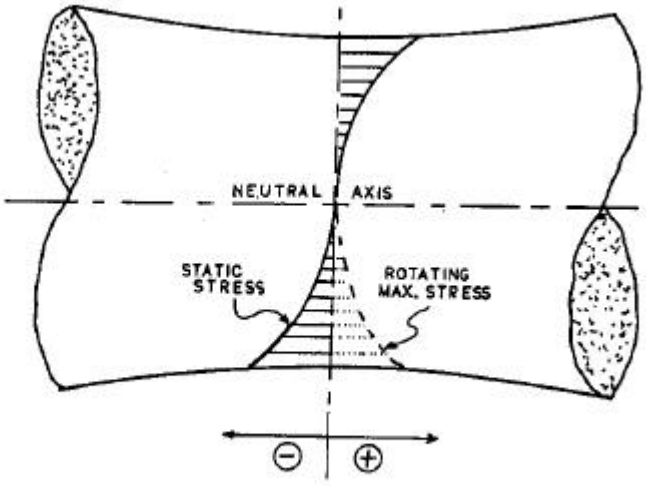

Figure 7: Stress distribution in a rotating bending fatigue specimen.

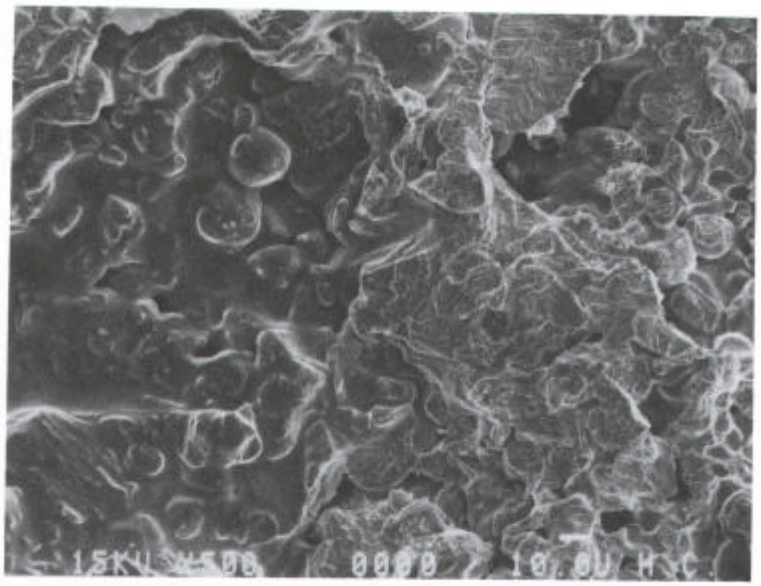

Figure 8: Transition between stable (left) and unstable (right) crack growth in an RBF specimen.

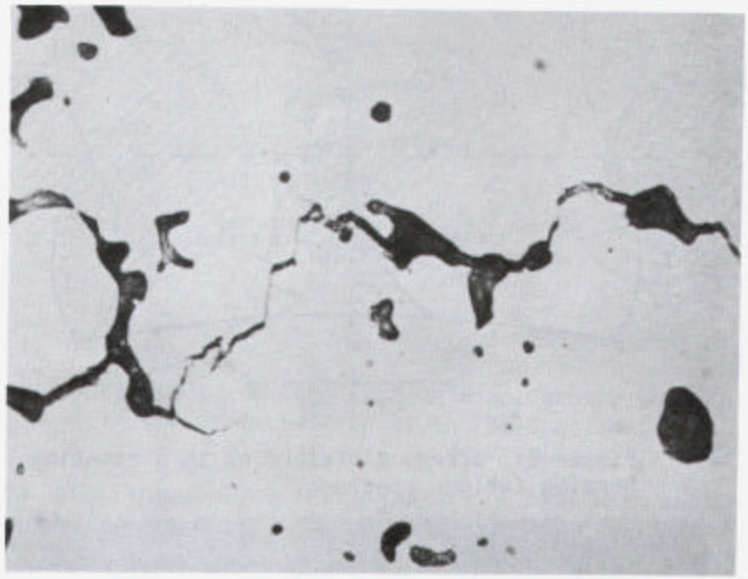

Figure 9: Crack propagation path in P/M steels. Crack follows the path of least resistance through pores.
1000X Unetched

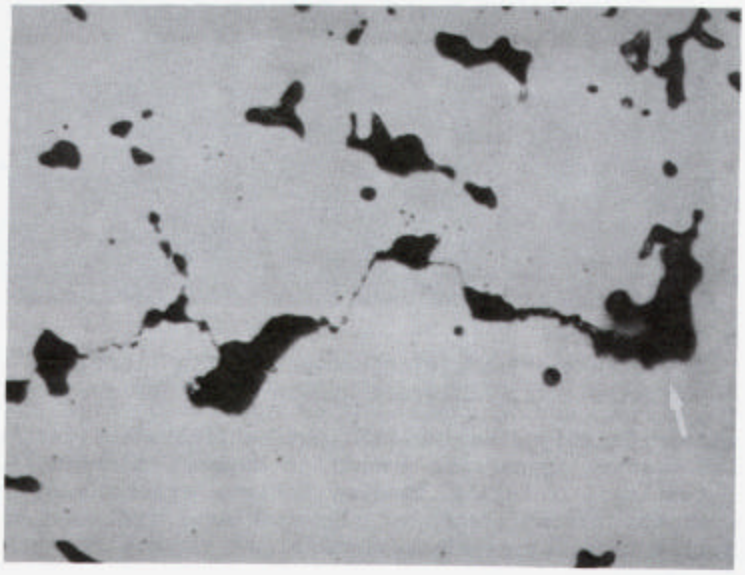

Figure 10: Crack propagation path in porous steels. Stable crack in Distaloy 4800A has ended in a pore.
1000X Unetched